

A Novel Route to Oscillations via non-central SNICeroclinic Bifurcation: unfolding the separatrix loop between a saddle-node and a saddle

Kateryna Nechyporenko^{1,2}, Peter Ashwin², and Krasimira Tsaneva-Atanasova^{1,2}

¹Living Systems Institute, University of Exeter, Stocker Road, Exeter EX4 4PY, UK

²Department of Mathematics and Statistics, University of Exeter, Harrison Building, Exeter EX4 4QF, UK

Abstract

In this paper, we investigate saddle–node to saddle separatrix-loops that we term SNICeroclinic bifurcations. There are generic codimension-two bifurcations involving a heteroclinic loop between one non-hyperbolic and one hyperbolic saddle. A particular codimension-three case is the non-central SNICeroclinic bifurcation. We unfold this bifurcation in the minimal dimension (planar) case where the non-hyperbolic point is assumed to undergo a saddle-node bifurcation. Applying the method of Poincaré return maps, we present a minimal set of perturbations that captures all qualitatively distinct behaviours near a non-central SNICeroclinic loop. Specifically, we study how variation of the three unfolding parameters leads to transitions from a heteroclinic and homoclinic loops; saddle-node on an invariant circle (SNIC); and periodic orbits as well as equilibria. We show that although the bifurcation has been largely unexplored in applications, it can act as an organising center for transitions between various types of saddle-node and saddle separatrix loops. It is also a generic route to oscillations that are both born and destroyed via global bifurcations, compared to the commonly observed scenarios involving local (Hopf) bifurcations and in some cases a global (homoclinic or SNIC) and a local (Hopf) bifurcation.

Keywords: Global bifurcations driving oscillatory patterns, Saddle separatrix-loops, Mechanisms of self-sustained oscillations; Dynamical systems in interdisciplinary research, Non-hyperbolic heteroclinic loop

AMS: 92B25, 34C15, 34C23, 34C37

1 Introduction

Saddle-node separatrix loops involving homoclinic and heteroclinic connections are important for understanding dynamical systems and their applications. For example, homoclinic bifurcations have been implicated in the control of different types of dynamic behaviour including periodic solutions in climate models [1, 2], lasers [3–5] and biochemical models [6, 7] as well as neurodynamics [8, 9]. Meanwhile, heteroclinic dynamics has been implicated in studies of information flow in cognitive processes [10, 11], decision making [12], memory [13] and attention [14]. However, most of the applications (especially of heteroclinic dynamics) have examined the bifurcation problems of orbits that are connected via hyperbolic equilibria, while the case of non-hyperbolic equilibria has received significantly less attention.

In particular, there has been a body of previous work focusing on the saddle-node homoclinic loop (SNHL) bifurcation (or saddle-node separatrix loop), a codimension-2 bifurcation of two-dimensional vector fields which represents a saddle-node whose separatrix forms a closed curve in the boundary of the two-dimensional invariant manifold [15]. This bifurcation has been introduced for the first time in the work of Luk'yanov [16] followed by Schechter [17] who performed an analytical study of the planar case using Mel'nikov functions. The results were generalised for any finitely-dimensional system by Chow and Lin in [18] applying a variety of techniques (exponential dichotomy; Melnikov function; smooth foliation; and Shil'nikov's central ideal). Their work appeared in parallel with further analysis in [19] aiming to unify the methods for studying homoclinic bifurcations.

Non-central saddle-node homoclinic (NCH) (another name found in literature describing SNHL) bifurcations can be found in biochemical systems, such as a model of GTPase activation [20], chemical reaction-diffusion system [21], and mathematical model of biochemical reactions [22]. Maruyama et al. [23] identified the presence of SNHL in the Wilson-Cowan model and demonstrated that, in a system of strongly coupled components (two interconnected Wilson-Cowan models), it can serve as a mechanism to induce chaos (aperiodic oscillations). Similar implications for chaos induction via SNHL are discussed in [1] where a simple model of atmospheric circulation is analysed. A study by [5] also reports this bifurcation as an organizing center of multipulse excitability in the injection laser. Later codimension-two global bifurcations were studied to understand the transitions to excitability, identifying both homoclinic and heteroclinic structures [4]. All these studies showcase the birth and disappearance of oscillations via global separatrix-loop bifurcations, such as SNIC and homoclinic in contrast to the more common case of a local Hopf bifurcation. However, heteroclinic bifurcation with at least one non-hyperbolic equilibria is less discussed in the literature in the context of oscillations.

The review [24, Section 5.2.3] includes a discussion of heteroclinic orbits with non-hyperbolic equilibria. They remark that a cycle including one saddle-node and one hyperbolic saddle (that we call here 'SNICeroclinic') will be generic for two parameter families, and that a cycle between two saddle-nodes may even perturb to infinitely many periodic orbits. In [25] unfolding of central heteroclinic loop between saddle node and saddle (here central SNICeroclinic) is presented, where the phenomenon is referred to as 'half-apple' bifurcation. In another paper, Dumortier et al. [26] considers the unfolding of the heteroclinic loop between saddle-node and saddle in two- and three-parameter family features saddle-node to saddle heteroclinic loop with non-central connection. This paper focuses on the cyclicity in the system, rather than heteroclinic structures as a route to oscillatory dynamics and does not highlight the applicability of the saddle-node to saddle heteroclinic loop with non-central connection.

In this paper, we are interested in revealing the types and bifurcations of saddle-node separatrix loops that can occur in minimal dimensions, regardless of specific details, helping to classify and understand these transitions. To this end we study the unfolding of a non-central SNICeroclinic loop between one hyperbolic and one non-hyperbolic saddle equilibria, where the non-hyperbolic equilibrium undergoes a saddle-node bifurcation. We carry out our analysis in a two-dimensional setting as this is the simplest scenario in which this bifurcation could occur but note additional features that will appear in higher dimensions. This codimension-three generic bifurcation includes the SNICeroclinic loop as a codimension two bifurcation in its neighbourhood.

We motivate the analysis presented below by exhibiting two examples of non-central SNICeroclinic loops in dynamical systems (see section 2). Then in our analysis we employ the method of Shilnikov variables [27], reducing the study of a continuous system to studying the associated discrete maps, referred to as a Poincaré map [28]. In section 3 we present the method of the construction of the Poincaré maps for the non-central SNICeroclinic loop, splitting the heteroclinic loop into two local and two global dynamics maps. Then in section 4 we consider the dynamics of the before, after and at the saddle-node bifurcation of the non-hyperbolic equilibrium.

2 Examples of non-central SNICeroclinic loops

A non-central SNICeroclinic loop is a heteroclinic loop connecting a hyperbolic and a non-hyperbolic saddle equilibrium, where the orbit approaching the non-hyperbolic saddle is non-central. In this section we give two simple motivating examples of non-central SNICeroclinic loops in two-dimensional dynamical systems. We note there are different types depending on whether the non-central eigenvalue ρ at the saddle-node is stable or unstable and whether the stable $-\lambda_s$ or unstable λ_u eigenvalue of the saddle dominates. Table 1 highlights the four possible cases.

	$\lambda_s > \lambda_u$	$\lambda_s < \lambda_u$
$\rho < 0$	Type I (stable)	Type II (mixed)
$\rho > 0$	Type III (mixed)	Type IV (unstable)

Table 1: Cases of the planar non-central SNICeroclinic loop bifurcation where ρ is the non-central eigenvalue of the saddle-node and $-\lambda_s$, λ_u are the eigenvalues of the saddle. In this paper we concentrate on the stable case Type I and the unstable case Type IV which corresponds to time-reversal of Type I.

2.1 A stable non-central SNICeroclinic loop in a polynomial singular fast-slow system

A non-central SNICeroclinic loop can be realised in the following two-dimensional polynomial fast-slow system of differential equations:

$$\begin{aligned} \dot{x} &= \epsilon(g(x) - y) \\ \dot{y} &= (x - f(y)), \end{aligned} \tag{1}$$

where $f(x)$ and $g(y)$ are

$$f(y) = -y^3 - 3y \tag{2}$$

$$g(x) = ax^2 + bx + c. \tag{3}$$

The parameter ϵ represents the separation of timescales between the "fast" (y) and "slow" (x) variables. By suitable choice of a , b and c , one can ensure in the singular limit $\epsilon \rightarrow 0$ that there are saddle-node p_{q1} and saddle p_2 equilibria as shown in Figure 1, where a separatrix entering p_{q1} approaches in a non-central direction and there is also a connection from p_{q1} to p_2 .

One can analytically determine parameters in the singular limit ($\epsilon \rightarrow 0$) under which the system exhibits a non-central SNICeroclinic loop. We do so by considering the nullcline geometry. There need to be saddle-node and saddle equilibria at drop points from the folds of the critical manifold $x = f(y)$, hence the saddle-node p_{q1} is at $(x, y) = (-2, -2)$, while saddle point p_2 is at $(x, y) = (2, 2)$. For the connections $p_{q1} \rightarrow p_2$ and $p_2 \rightarrow p_1$ to exist the x -nullcline must be zero at p_{q1} and p_2 , respectively. This gives us two equations $-2 = 4a + 3b + c$ and $2 = 4a + 3b + c$ for the x -nullcline. For p_{q1} to be a saddle-node we need the x - and y -nullclines to be tangent at p_{q1} meaning that $2ax + b|_{p_{q1}} = -4a + b = 1/9$. Solving these three constraints we find a non-central SNICeroclinic loop at $(a, b, c) = (0.222\bar{2}, 1, 0.888\bar{8})$ for the polynomial system in singular limit. These equilibria and connections will be robust under small perturbations of ϵ if we change (a, b, c) , meaning there is a curve of parameters $(a(\epsilon), b(\epsilon), c(\epsilon))$, such that a non-central SNICeroclinic loop exists in the system for any small enough $\epsilon > 0$. In the polynomial system we demonstrate existence of a SNICeroclinic loop at $\epsilon = 1$ (see Figure 1(A)). This is an example of Type I non-central SNICeroclinic loop. We

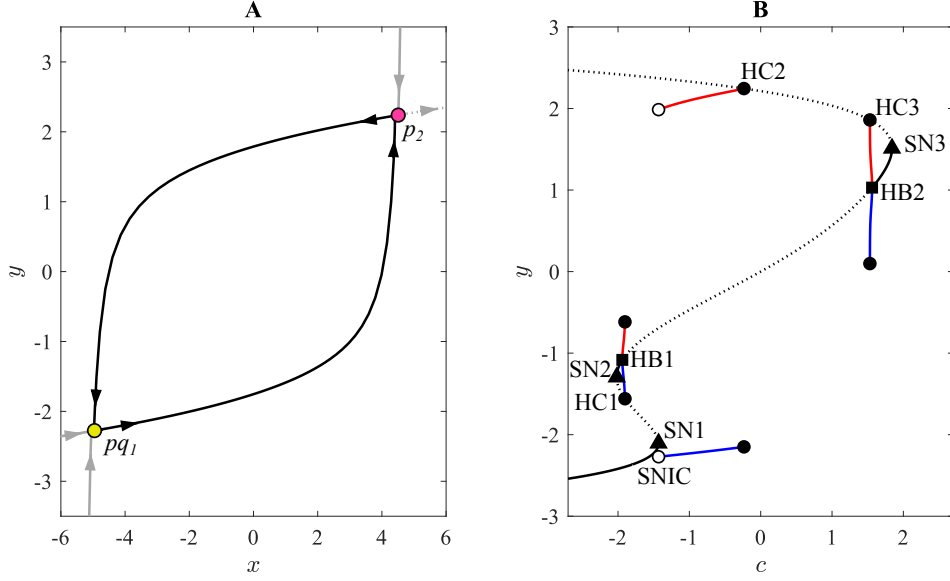


Figure 1: **(A)** Non-central SNICeroclinic loop in the polynomial system Equation 1 with $\epsilon = 1$, $a = 0.042$, $b = 0.49575$ and $c = -0.85$. Yellow and pink circles identify saddle-node and saddle, respectively. Black line shows the SNICeroclinic loop between the saddle-node and saddle, grey lines signify the direction of the manifolds of each of the equilibria. Solid and dotted grey lines identify stable and unstable manifolds, respectively. **(B)** Continuation in the parameter c in the polynomial system ($\epsilon = 1$, $a = 0.042$, $b = 0.35$), where solid and dotted black lines identify stable and unstable equilibria, respectively; red and blue lines show the maximum and the minimum of the periodic solutions, respectively; black triangle (SN1, SN2, SN3): saddle node; black square (HB1, HB2): Hopf; black circle (HC1, HC2, HC3): homoclinic; white circle (SNIC): saddle node on invariant circle.

compute one-parameter bifurcation diagram in c , which illustrates a limit cycle born through a SNIC bifurcation, while its destruction occurs via a homoclinic (see Figure 1(B)). This suggests a novel route to oscillations, where periodic solutions appear and disappear via global bifurcations, namely SNIC and homoclinic.

2.2 An unstable non-central SNICeroclinic loop in a GTPase activation model

If the saddle-node has positive, non-zero eigenvalue, resulting in a linearly unstable direction. We demonstrate this case of an unstable SNICeroclinic loop using the GTPase-tension model of [20, 29] given by the following ODEs:

$$\begin{aligned} \frac{dL}{dt} &= -\varepsilon(L - L_0(G, \phi_1)) \\ \frac{dG}{dt} &= \left(b + f(L) + \gamma \frac{G^n}{1 + G^n} \right) (G_T - G) - G, \end{aligned} \quad (4)$$

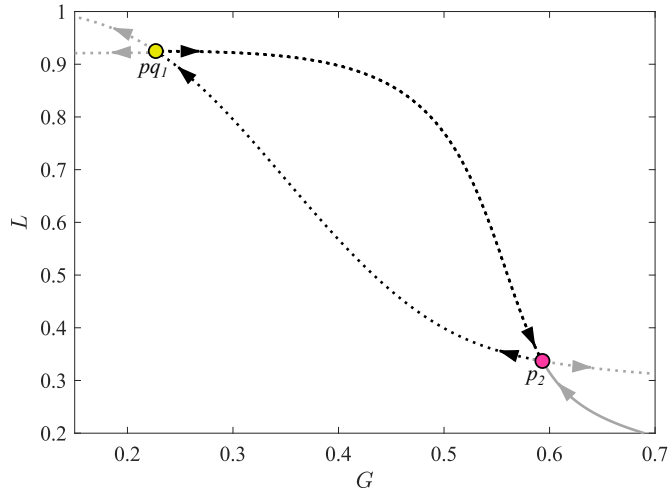


Figure 2: A non-central SNICeroclinic loop between a saddle-node pq_1 with linearly unstable direction and saddle p_2 in the GTPase activation model Equation 4. Yellow and pink circles identify saddle-node and saddle, respectively. Black dotted line shows the unstable SNICeroclinic loop between the saddle-node and the saddle, solid and dotted grey lines signify the stable and unstable manifolds, respectively.

where G and L depict the GTPase concentration and cell size, respectively. The function $f(L)$ is a mechanical feedback mechanism from cell deformation to GTPase activity. In [29] different forms of f under different assumptions have been considered. For the purposes of our analysis we have selected the Hill function:

$$f(L) = \beta \frac{L^m}{L_0(G, \phi_2)^m + L^m}. \quad (5)$$

The term L_0 represents the rest length that is assumed to decrease from the original length ℓ_0 depending on the amount of active GTPase in the cell:

$$L_0 = L_0(G, \phi) = \ell_0 - \phi \frac{G^p}{G_h^p + G^p}, \quad (6)$$

where the parameter ϕ is the scaled rate of the GTPase activation. For our analysis we assume that the GTPase concentration and cell size integrate the active GTPase differently, hence we use ϕ_1 and ϕ_2 to represent it. The detailed description of the model can be found in [20, 29]. The parameters used to achieve a non-central SNICeroclinic in the GTPase activation model are in Table 2. The nonhyperbolic point has an unstable non-zero eigenvalue, and, as a result, the heteroclinic connections will be formed on the intersection of the unstable manifold of the saddle and stable central manifold of the saddle-node as well as the intersection of the stable manifold of the saddle and unstable manifold of the saddle-node. Moreover, the unstable eigenvalue dominates the stable eigenvalue of the saddle. This means we have an unstable (Type IV in Table 1) non-central SNICeroclinic loop. The non-central entrance in the neighbourhood of the saddle-node equilibrium arises inherently. Otherwise, the flow will leave the neighbourhood of the SNICeroclinic loop, prompted by the unstable separatrix. The below unfolding of a codimension three saddle–node to saddle separatrix-loop bifurcation can be applied to this scenario by reversing time.

Parameter	Value	Description
β	0.0052	strength of feedback from tension to GTPase activation
b	0.2530	basal activation rate
γ	1.6	scaled rate of feedback activation
G_T	2	mechanical activation constant
ℓ_0	1	rest length
ϕ_1	0.9	Hill function amplitude
ϕ_2	2	Hill function amplitude
G_h	0.4	half-maximum GTPase activity
ϵ	0.1	rate of contraction
n, p, m	4	Hill coefficients

Table 2: Model parameters for the GTPase activation model Equation 4.

3 The non-central SNICeroclinic loop bifurcation

We consider this as an identification problem in general dimensions before giving an unfolding for the planar case.

3.1 The general non-central SNICeroclinic loop

Consider an n -dimensional dynamical system given by differential equations:

$$\frac{du}{dt} = f(u) \quad u \in \mathbb{R}^n, \quad (7)$$

where $f : \mathbb{R}^n \rightarrow \mathbb{R}^n$ is C^r ($r \geq 2$). Assume that Equation 7 has a nonhyperbolic equilibrium p_{q1} , a hyperbolic saddle p_2 and connections between them as in Figure 3(A).

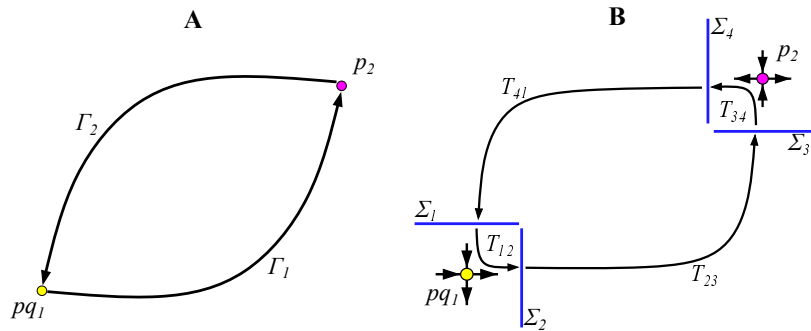


Figure 3: (A) Non-central SNICeroclinic loop $\Gamma = \overline{\Gamma_1 \cup \Gamma_2}$ between saddle-node p_{q1} and saddle p_2 . (B) Overview of the construction of the Poincaré map for the planar case in the vicinity of the heteroclinic loop Γ between nonhyperbolic equilibrium (p_{q1} , yellow) and hyperbolic saddle (p_2 , pink) with established cross-sections ($\Sigma_1, \Sigma_2, \Sigma_3, \Sigma_4$) and corresponding ‘‘connection’’ maps $T_{12}, T_{23}, T_{34}, T_{41}$.

More precisely, assume p_{q1} and p_2 are connected via a heteroclinic loop formed by the separatrices

Γ_1 and Γ_2 (see Figure 3(A,B)):

$$\Gamma_1 := \{z = u(t), t \in \mathbb{R} \mid u(+\infty) = p_2 \text{ and } u(-\infty) = pq_1\} \quad (8)$$

$$\Gamma_2 := \{z = u(t), t \in \mathbb{R} \mid u(+\infty) = pq_1 \text{ and } u(-\infty) = p_2\}. \quad (9)$$

We consider the heteroclinic contour formed by $\Gamma = \overline{\Gamma_1 \cup \Gamma_2}$ and are interested in the invariant sets and bifurcations that appear within some neighbourhood \mathcal{U} of Γ . We say Γ is a *non-central SNICeroclinic loop* if:

- H1*** The system Equation 7 has a generic saddle-node equilibrium pq_1 whose Jacobian $Df(pq_1)$ has simple eigenvalue 0 and all other eigenvalues lie on one side of the imaginary axis.
- H2*** The system has a saddle equilibrium p_2 whose Jacobian $Df(p_2)$ has leading eigenvalues λ_u and λ_s , with $\Re(\lambda_u) > 0$ and $\Re(\lambda_s) < 0$.
- H3*** There is a single trajectory Γ_1 from pq_1 to p_2 that is a generic intersection of invariant manifolds.
- H4*** There is a single trajectory Γ_2 from p_2 to pq_1 that is a generic intersection of invariant manifolds.
- H5*** Γ_2 approaches pq_1 , or Γ_1 leaves pq_1 in a non-central direction.
- H6*** We assume the eigenvalues of pq_1 and p_2 , and any intersections of invariant manifolds are in general position given the constraints above.

If **H5*** is not satisfied, but **H1*-H4*** are, then we say Γ is a *SNICeroclinic loop*. We simplify these assumptions and consider an unfolding in the special case $n = 2$ in the next section. Challenges associated with the general unfolding problem are discussed in section 5.

3.2 Unfolding the planar case

Now consider the parametrised planar dynamical system:

$$\frac{du}{dt} = f(u, \mu) \quad (u, \mu) \in \mathbb{R}^2 \times \mathbb{R}^3, \quad (10)$$

where $f : \mathbb{R}^2 \times \mathbb{R}^3 \rightarrow \mathbb{R}^2$ is C^r ($r \geq 2$). We will unfold this using the Kuznetsov Normal Form Theorem [30] to locally approximate the system near the non-central SNICeroclinic loop and then proceed to construct a Poincaré map. Construction of the Poincaré map involves a reduction to a co-dimension one surface where we preserve local dynamics of the original system [31]. We follow the method of [26] but we try to make the assumptions and calculations more explicit and generalizable to higher dimensional cases.

In the planar case $n = 2$ we assume there is a Γ with neighbourhood \mathcal{U} such that **H1*-H6*** become the following hypotheses for $\mu = 0$:

- H1** The system Equation 10 has an equilibria pq_1 whose Jacobian $Df(pq_1)$ has real eigenvalues $\rho \neq 0$ and 0. This is a generic saddle-node.
- H2** The system has an equilibrium p_2 whose Jacobian $Df(p_2)$ has two simple real eigenvalues: $\lambda_u > 0$ and $\lambda_s < 0$.
- H3** The one-dimensional center $W^c(pq_1)$ contains a trajectory Γ_1 that limits to p_2 .

H4 The one-dimensional unstable $W^u(p_2)$ contains a trajectory Γ_2 the limits to pq_1 .

H5 Γ_2 approaches pq_1 in a non-central direction.

H6 We have $\lambda_s \neq \lambda_u$.

In addition we assume **H7**: The parametrization by μ is in general position and this unfolds the bifurcation at $\mu = 0$.

As for the general case, if **H5** is not satisfied but **H1-4** are, then we say Γ is a SNICeroclinic loop; this will be generic in two parameter families [25]. Even in the planar case, there are several types of non-central SNICeroclinic loop in the plane, depending on the sign of ρ and $\lambda_s - \lambda_u$, as outlined in Table 1. In this paper, we concentrate on stable case Type I which results in bifurcation to attracting periodic orbits. The unstable case Type IV corresponds to the case with saddle-node with linearly unstable direction, the existence of which was demonstrated in the GTPase activation model. The unfolding of the mixed cases Type II and Type III can be found in [26] and include both stable and unstable periodic orbits that meet at a saddle node of periodic orbits.

We perform geometric decomposition of the heteroclinic loop using local and global maps to derive the conditions for different bifurcations to occur varying the parameters μ . We argue that the considered non-central SNICeroclinic loop is a codimension-three structure, where one parameter is responsible for the saddle-node bifurcation of pq_1 , and two other parameters control the bifurcation of the trajectories Γ_1 and Γ_2 . Let μ_1 to be an unfolding parameter of the saddle-node bifurcation of pq_1 and the parameters μ_2 and μ_3 to be as the splitting parameters for separatrices Γ_1 and Γ_2 , respectively. We separate the heteroclinic loop Γ into 4 segments with distinct qualitative dynamics (see Figure 3(B)). The maps T_{12} and T_{34} are local maps around points pq_1 and p_2 , respectively, while the maps T_{23} and T_{41} are the global transition maps from neighbourhood U_1 to U_2 and from U_2 to U_1 , respectively.

3.3 Local map around saddle-node pq_1 : T_{12}

According to the center manifold theory there exists a center manifold that governs the flow on a small neighbourhood of pq_1 [32]. We use the saddle-node normal form to define the unfolding of local dynamics around the box neighbourhood $U_1 := \{(x, y) \in \mathbb{R}^2 \mid |x|, |y| \leq \delta\} \subset \mathcal{U}$ of the critical point pq_1 , where $\delta \ll 1$ [33, 34]. Under this choice of variables, the flow is as follows:

$$\dot{x} = x^2 - \mu_1 \tag{11}$$

$$\dot{y} = \rho y, \tag{12}$$

where μ_1 is the unfolding parameter. We use method of Shil'nikov variables [27] to find the transition map from Σ_1 to Σ_2 . Let us define the cross-sections as follows:

$$\Sigma_1 := \{(x, y) \in \mathbb{R}^2 \mid |x| < \delta, y = \delta\} \tag{13}$$

$$\Sigma_2 := \{(x, y) \in \mathbb{R}^2 \mid |y| < \delta, x = \delta\}. \tag{14}$$

We suppose that at time $t = 0$ the flow intersects Σ_1 at $x = x_0 > 0$ and at time $t = \tau$ it intersects Σ_0 at $y = y_1 > 0$. We have three cases: $\mu_1 > 0$, $\mu_1 < 0$ and $\mu_1 = 0$.

- *Case 1: $\mu_1 < 0$*

For $\mu_1 < 0$ the system of equations (11) and (12) has no real fixed points, i.e. the saddle-node disappears for $\mu_1 < 0$. The general solution of the system of the equations (11) and (12) in

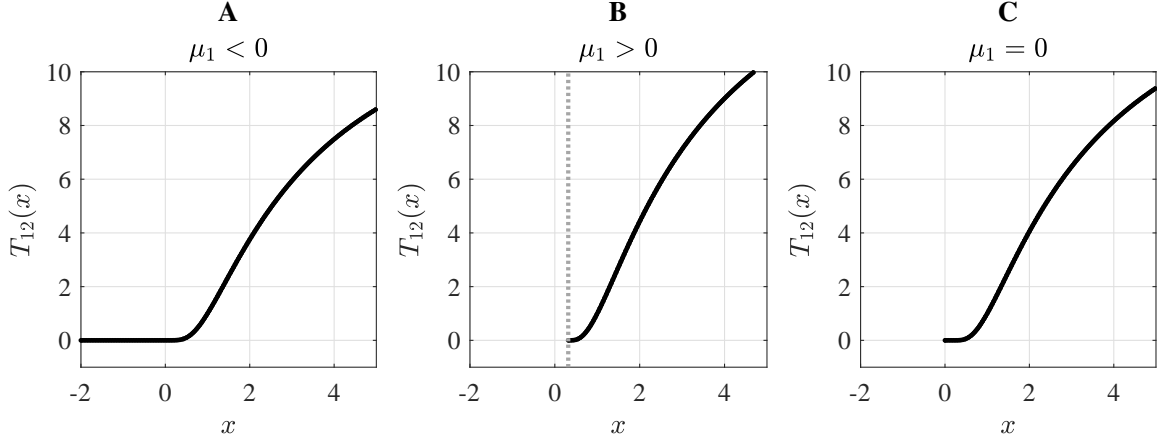


Figure 4: Representation of the connecting maps T_{12} for **(A)** $\mu_1 < 0$, **(B)** $\mu_1 > 0$, **(C)** $\mu_1 = 0$.

this case is the following:

$$t + C_1 = \frac{1}{\sqrt{|\mu_1|}} \arctan\left(\frac{x}{\sqrt{|\mu_1|}}\right) \quad (15)$$

$$y = C_2 e^{t\rho}, \quad (16)$$

where C_1 and C_2 are constants. Using initial conditions $(x_0, \delta) \in \Sigma_1$ we obtain

$$C_1 = \frac{1}{\sqrt{|\mu_1|}} \arctan\left(\frac{x_0}{\sqrt{|\mu_1|}}\right) \quad (17)$$

$$C_2 = \delta. \quad (18)$$

At $t = \tau$ we assume $(x, y) \in \Sigma_2$, thus we have $x = \delta$ and $y = y_1$, where $|y_1| < \delta$, yielding:

$$\tau = \frac{1}{\sqrt{|\mu_1|}} \left[\arctan\left(\frac{\delta}{\sqrt{|\mu_1|}}\right) - \arctan\left(\frac{x_0}{\sqrt{|\mu_1|}}\right) \right] \quad (19)$$

$$y_1 = \delta e^{\tau\rho}. \quad (20)$$

As τ must be positive we require $x_0 = \{x \in \mathbb{R} | x < \delta\}$. Substituting the expression for τ in equation 19 into 20 we obtain the expression for transition map T_{12} (see Figure 4**(A)**):

$$T_{12} = \delta \exp \left[\frac{\rho}{\sqrt{|\mu_1|}} \left(\arctan\left(\frac{\delta}{\sqrt{|\mu_1|}}\right) - \arctan\left(\frac{x_0}{\sqrt{|\mu_1|}}\right) \right) \right] \quad (21)$$

At small values of $x < 0$ the map T_{12} approaches zero, but never equal to it.

- *Case 2: $\mu_1 > 0$*

The linearised system for $\mu_1 > 0$ has two fixed points - one stable $(-\sqrt{\mu_1}, 0)$ and hyperbolic saddle $(\sqrt{\mu_1}, 0)$. We refer to the saddle point as p_1 . The general solution of the system of the

equations (11) and (12) with positive μ_1 is

$$t + C_1 = \frac{1}{2\sqrt{\mu_1}} \ln \left| \frac{x - \sqrt{\mu_1}}{x + \sqrt{\mu_1}} \right| \quad (22)$$

$$y = C_2 e^{t\rho}, \quad (23)$$

where C_1 and C_2 are constants. Using initial conditions $(x_0, \delta) \in \Sigma_1$ we obtain

$$C_1 = \frac{1}{2\sqrt{\mu_1}} \ln \left| \frac{x_0 - \sqrt{\mu_1}}{x_0 + \sqrt{\mu_1}} \right| \quad (24)$$

$$C_2 = \delta. \quad (25)$$

At $t = \tau$ we hit $(\delta, y_1) \in \Sigma_2$, which yields:

$$\tau = \frac{1}{2\sqrt{\mu_1}} \left[\ln \left| \frac{\delta - \sqrt{\mu_1}}{\delta + \sqrt{\mu_1}} \right| - \ln \left| \frac{x_0 - \sqrt{\mu_1}}{x_0 + \sqrt{\mu_1}} \right| \right] \quad (26)$$

$$y_1 = \delta e^{\tau\rho}. \quad (27)$$

As τ must be positive we require $x_0 = \{x \in \mathbb{R} | \sqrt{\mu_1} \leq x < \delta\}$, putting restrictions on Σ_1 . Substituting the expression for τ in equation (26) into (27) we obtain the expression for transition map T_{12} for $\mu_1 > 0$ (Figure 4(B)):

$$T_{12} = \delta \exp \left[\frac{1}{2\sqrt{\mu_1}} \left[\ln \left| \frac{\delta - \sqrt{\mu_1}}{\delta + \sqrt{\mu_1}} \right| - \ln \left| \frac{x - \sqrt{\mu_1}}{x + \sqrt{\mu_1}} \right| \right] \right]. \quad (28)$$

Note, we restrict the domain of the 'connecting' map T_{12} for $\mu_1 > 0$ to be $x \in (\sqrt{\mu_1}, \delta)$.

- *Case 3: $\mu_1 = 0$*

When $\mu_1 = 0$, the linearised system has one non-hyperbolic saddle point $(0, 0)$.

The general solution of the system of the equations 11 and 12:

$$t + C_1 = -\frac{1}{x} \quad (29)$$

$$y = C_2 e^{t\rho}, \quad (30)$$

where C_1 and C_2 are constants. Using initial conditions we obtain

$$C_1 = -\frac{1}{x_0} \quad (31)$$

$$C_2 = \delta. \quad (32)$$

At $t = \tau$ we have $x = \delta$ and $y = y_1$, yielding:

$$\tau = \frac{1}{x_0} - \frac{1}{\delta} \quad (33)$$

$$y_1 = \delta e^{\tau\rho}. \quad (34)$$

As τ must be positive we require $x_0 = \{x \in \mathbb{R} | 0 \leq x < \delta\}$. This imposes restriction to the Σ_1 . Substituting the expression for τ in equation 33 into 34 we obtain the expression for transition map T_{12} (see Figure 4(C)):

$$T_{12}(x) = \delta \exp \left[\rho \left(\frac{1}{x} - \frac{1}{\delta} \right) \right] \quad (35)$$

3.4 Local map around saddle point p_2 : T_{34}

Using Grobman-Hartman theorem [27], we can assume that a smooth coordinate change has been undertaken that flattens the stable and unstable manifolds within a small box neighbourhood U_2 of p_2 . We assume that within U_2 the dynamics is completely linear. We choose to omit higher order terms here, as our aim is to achieve a plausible argument for asymptotic scaling.

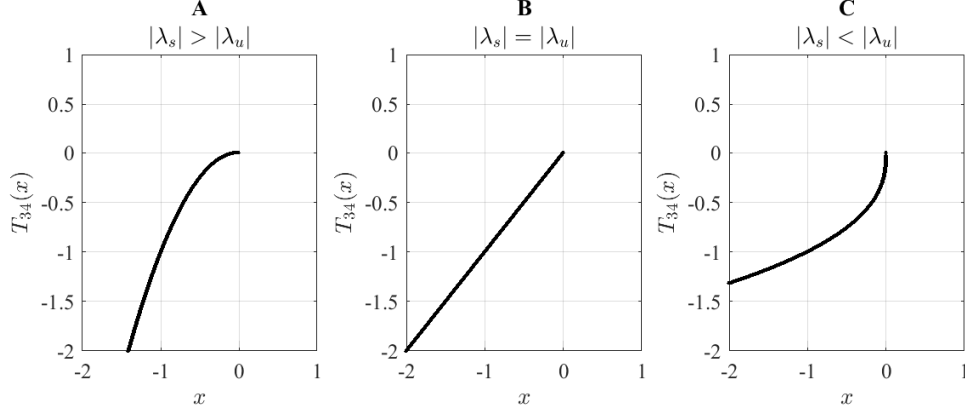


Figure 5: Representation of the connecting maps T_{34} for **(A)** $|\lambda_s| > |\lambda_u|$, **(B)** $|\lambda_s| = |\lambda_u|$, **(C)** $|\lambda_s| < |\lambda_u|$.

We set local coordinate system within U_2 $(x, y)^T$, such that the linear system can be written:

$$\dot{x} = \lambda_u x \tag{36}$$

$$\dot{y} = \lambda_s y. \tag{37}$$

In this coordinate system, the dynamics in the local stable $W_{loc}^s(p_2)$ and unstable manifolds $W_{loc}^u(p_2)$ correspond to the uncoupled subsystems associated with eigenvalues of λ_s and λ_u , respectively.

Under the construction, x (y) is in the direction of unstable (stable) manifolds. Without loss of generality, choose a box U_2 in the form:

$$U_2 := \{(x, y) \in \mathbb{R}^2 \mid |x|, |y| \leq \epsilon\}, \quad \text{for some } \epsilon \ll 1. \tag{38}$$

We can now define the Poincaré sections on dU_2 :

$$\Sigma_3 := \{(x, y) \in \mathbb{R}^2 \mid |x| < \epsilon, y = -\epsilon\} \tag{39}$$

$$\Sigma_4 := \{(x, y) \in \mathbb{R}^2 \mid |y| < \epsilon, x = -\epsilon\}. \tag{40}$$

These sections are transverse to the flow provided $|\epsilon|$ is small enough. Obviously, the trajectories, which stays for all positive times in the neighbourhood U_2 of the heteroclinic loop must intersect Σ_3 and Σ_4 . Using the method of Shil'nikov variables [27], we can find a transition map $T_{34} : \Sigma_3 \rightarrow \Sigma_4$ near equilibrium by solving a boundary value problem for the system of equations (36) and (37). We emphasise these boundary conditions ensure that the flow is to stay in the closure of Γ .

In the neighbourhood of U_2 let the trajectory start at $(x_0, -\epsilon) \in \Sigma_3$ and end at $(-\epsilon, y_1) \in \Sigma_4$. The general solution to the system of equations (36) and (37) is

$$x = C_1 e^{\lambda_u t} \quad (41)$$

$$y = C_2 e^{\lambda_s t}, \quad (42)$$

where $C_1, C_2 \in \mathbb{R}$. Using initial conditions $(x, y) = (x_0, -\epsilon)$ at $t = 0$, we obtain $C_1 = x_0$ and $C_2 = -\epsilon$. Consider the system at $t = \tau$:

$$-\epsilon = x_0 e^{\lambda_u \tau} \quad (43)$$

$$y_1 = -\epsilon e^{\lambda_s \tau}. \quad (44)$$

Rearranging the terms in equation 43 we obtain:

$$\tau = \frac{1}{\lambda_u} \ln \frac{\epsilon}{|x_0|}. \quad (45)$$

We note that the expression for τ is defined only for $-\epsilon < x_0 \leq 0$. Substituting expression for τ in equation (45) into equation (44) we obtain the transition map T_{34} :

$$T_{34}(x) = -\epsilon^{1+\lambda_s/\lambda_u} |x|^{-\lambda_s/\lambda_u}, \quad (46)$$

which is defined for $-\epsilon < x \leq 0$. We note that evolution of the system is defined by the point at which the trajectory enters the local neighbourhood of p_2 , specifically:

- if the trajectory enters Σ_3 at $-\epsilon < x_0 < 0$, it will stay in the neighbourhood \mathcal{U} of Γ after leaving the local neighbourhood of p_2
- if the trajectory enters Σ_3 at $x_0 = 0$, it will tend to p_2 , then will leave the neighbourhood U_2 .
- if the trajectory enters Σ_3 at $x_0 > 0$, it will leave the neighbourhood \mathcal{U} of Γ without passing through the saddle point p_2 .

Furthermore, based on the magnitude of λ_s/λ_u the shape of the connecting map T_{34} changes (see Figure 5). The magnitude of the eigenvalue of the saddle point tells us how fast the flow travels in that direction [30]. In our analysis we only consider the case when $\lambda_s > \lambda_u$, depicted in Figure 5(A).

3.5 Global maps: T_{23} and T_{31}

We want to define the global dynamics that governs the flow that starts at the cross-section Σ_2 and ends at the cross-section Σ_1 . We separate the flow into two parts - the flow that goes from the neighbourhood of p_{q1} and ends at the neighbourhood of p_2 and the flow that starts at the neighbourhood of p_2 and goes to the neighbourhood of p_{q1} (Figure 3(B)). The cross-section Σ_3 , which is transverse to the flow, separates them. To approximate the flow from Σ_2 to Σ_3 we use polynomial approximation of the path for the system in (10) at x_0 (y component of the cross-section Σ_2):

$$T_{23}(x) = a_1 x + \mu_2 + O(|x|^2), \quad (47)$$

where a_1 is a constant and μ_2 is an unfolding parameter. We set the

Similarly, the flow from Σ_3 to Σ_1 is approximated as

$$T_{41}(x) = a_2x + \mu_3 + O(|x|^2), \quad (48)$$

where a_2 is a constant and μ_3 is an unfolding parameter. As in the neighbourhood of p_{q1} we consider only non-negative values, while in the neighbourhood of p_2 we restrict the map to negative values, we use global maps T_{23} and T_{41} to preserve the transition between positive and negative values by fixing $a_1 = a_2 = -1$.

3.6 Return maps

Using the connecting maps T_{12} , T_{23} , T_{34} , T_{41} we can define return maps to each cross-section:

$$R_1 = T_{41} \circ T_{34} \circ T_{23} \circ T_{12}(x) \text{ to } \Sigma_1, \quad (49)$$

$$R_2 = T_{12} \circ T_{41} \circ T_{34} \circ T_{23}(x) \text{ to } \Sigma_2, \quad (50)$$

$$R_3 = T_{23} \circ T_{12} \circ T_{41} \circ T_{34}(x) \text{ to } \Sigma_3, \quad (51)$$

$$R_4 = T_{34} \circ T_{23} \circ T_{12} \circ T_{41}(x) \text{ to } \Sigma_4. \quad (52)$$

3.7 Analysis method

We observe that in our system with a saddle-node and a saddle point the behaviour in the neighbourhood \mathcal{U} of Γ depends on the behaviour of separatrices Γ_1 and Γ_2 . In [35] a lemma was proposed that showed that in the unfolding of the heteroclinic loop between two saddle-foci any orbit that stays in the neighbourhood of the heteroclinic loop lies in the closure of the union of separatrices connecting the points. Particularly, it implies that the behaviour of the trajectories, which start within the neighbourhood of heteroclinic loop, is determined by the behaviour of the separatrices that are associated with each saddle. We apply this theoretical finding to our analysis. Specifically, we discuss the conditions to induce a specific qualitative behaviour in the system, then validate them by considering the stable fixed points of the return maps. The return maps' fixed points allows us to identify whether a separatrix leaves the neighbourhood \mathcal{U} of Γ or not. To this end we split our analysis of the parameter space of μ into three parts: $\mu_1 = 0$, $\mu_1 < 0$, $\mu_1 > 0$ -, as T_{12} is split into three cases. For each of the three cases for μ_1 we will analyse the dynamics in the system by considering return maps under variation of splitting parameters (μ_2, μ_3) . We start by fixing the parameter $\mu_1 = 0$.

4 Unfolding the non-central SNICeroclinic

4.1 Unfolding the case $\mu_1 = 0$

When $\mu_1 = 0$ the system has two fixed equilibria - a saddle-node and a saddle. Varying the splitting parameters μ_2 and μ_3 we aim to explore the range of distinct dynamic behaviours. It includes non-central and central heteroclinic connection between p_{q1} and p_2 , homoclinic loop with p_2 , non-central and central SNIC with p_{q1} , existence of periodic solutions with diverse behaviour of separatrices Γ_1 and Γ_2 as well as destruction of invariant structures. All scenarios on the parameter space (μ_2, μ_3) are demonstrated in Figure 6. In the following subsections, we will explore the necessary conditions for maintaining the persistence of a specific dynamic state within the system.

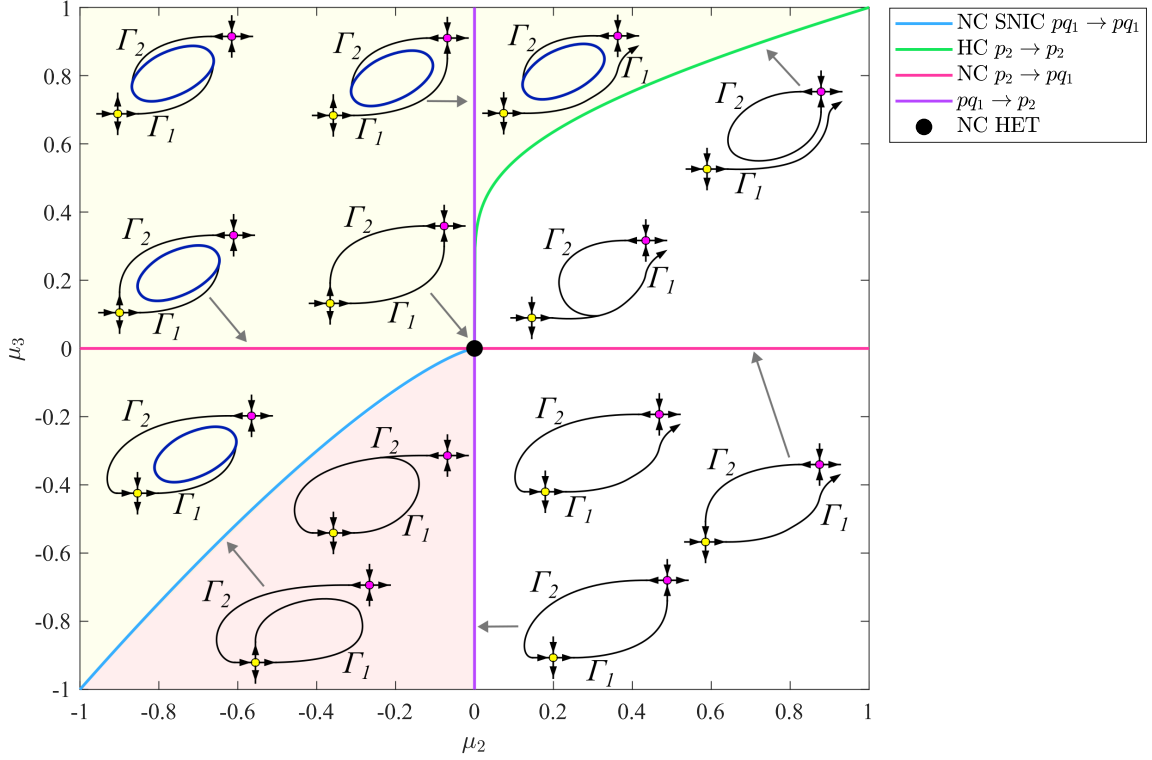


Figure 6: Unfolding of the heteroclinic loop between non-hyperbolic (yellow dot) and hyperbolic (pink dots) points. The parameter $\mu_1 = 0$ is fixed, while changes in parameters μ_2 and μ_3 alter the qualitative behaviour of the system. Black dot signifies the non-central heteroclinic loop, the curves separate the parameter regions of different dynamics as described in the legend. Yellow and white coloured regions signify the presence and absence of a periodic orbit, respectively, while red-coloured region indicates the existence of the central SNIC. The dynamics of the system is also illustrated via phase portraits, depicting the behaviour of the separatrices Γ_1 and Γ_2 . Dark blue closed curves identify the presence of a periodic orbit. SNIC: saddle-node on invariant circle, HC: homoclinic loop, HET: heteroclinic loop, NC: non-central.

4.1.1 At the non-central SNICeroclinic bifurcation

When defining the Poincaré maps we assumed that at $\mu = (0, 0, 0)$ there exists a heteroclinic loop between p_{q_1} and p_2 , which we define as the location of the SNICeroclinic bifurcation. In this case all the maps to each of the four cross-sections have a stable fixed point at $x = 0$ (see Figure 2), indicating the presence of the bidirectional heteroclinic connection between equilibria. Moreover, given the way we defined the maps if we fix $\mu_2 = 0$ and vary μ_3 we preserve heteroclinic connection $p_{q_1} \rightarrow p_2$ formed by Γ_1 . Depending on the sign of μ_3 we either will produce a persistence of a periodic orbit for $\mu_3 > 0$ or formation of central heteroclinic connection $p_2 \rightarrow p_{q_1}$. The later case will lead to the persistence of central heteroclinic loop. Similarly, if we fix $\mu_3 = 0$ and vary μ_2 we can preserve the persistence of non-central heteroclinic connection $p_2 \rightarrow p_1$, formed by Γ_2 . Then, if $\mu_2 < 0$ the separatrix Γ_1 stays in the neighbourhood \mathcal{U} , tending to a periodic orbit. If $\mu_2 > 0$, the separatrix Γ_1 leaves the neighbourhood \mathcal{U} .

4.1.2 Homoclinic loop $p_2 \rightarrow p_2$

The homoclinic orbit exists on the intersection of stable and unstable manifolds of the saddle p_2 . To ensure this condition in our return maps, the trajectories in the neighbourhood \mathcal{U} of Γ are to enter Σ_3 at a point $(0, \epsilon)$, thus we require the fixed point of the return map R_3 to be 0:

$$0 = R_3(0) \quad (53)$$

$$0 = a_1 T_{12}(\mu_3) + \mu_2 \quad (54)$$

$$\mu_2 = -a_1 T_{12}(\mu_3), \quad (55)$$

giving us the conditions on the parameters μ_2 and μ_3 . Additionally, the separatrix Γ_2 must not form the heteroclinic connection (both central and non-central), hence $\mu_3 > 0$. Under these conditions, the separatrix Γ_2 forms a homoclinic loop, while Γ_1 leaves the neighbourhood. If we set $\mu_2 > -a_1 T_{12}(\mu_3)$ the return map to the cross-section Σ_3 will lose a stable fixed point, indicating that the separatrix Γ_2 leaves the neighbourhood \mathcal{U} , uniting with the separatrix Γ_1 . On the other hand, if $\mu_2 < -a_1 T_{12}(\mu_3)$, the return maps have non-zero stable fixed points, demonstrating that the separatrix Γ_2 tends to a periodic orbit in the neighbourhood \mathcal{U} . Hence, the curve $\mu_2 = -a_1 T_{12}(\mu_3)$ for the homoclinic loop $p_2 \rightarrow p_2$ is the mechanism that induces transition between persistence of periodic solutions in the system and their destruction.

4.1.3 Non-central saddle-node on invariant circle (SNIC) $pq_1 \rightarrow pq_1$

The behaviour of manifolds in the context of SNIC is a complicated questions, as the relative position of the manifolds varies [24]. In the case when we have non-central SNIC stable and unstable-central manifolds conjoin, which is also consistent with what occurs at the SNHL bifurcation. To observe saddle-node on invariant circle (SNIC) $pq_1 \rightarrow pq_1$ we require the trajectories to enter the neighbourhood of pq_1 at $\Sigma_1 = (0, \delta)$, hence R_1 must have a fixed point at $x = 0$:

$$0 = R_1(0), \quad (56)$$

$$0 = a_2 T_{34}(\mu_2) + \mu_3, \quad (57)$$

$$\mu_3 = -a_2 T_{34}(\mu_2), \quad (58)$$

which defines the relationship between the splitting parameters. Additionally, we require the separatrix Γ_1 not to leave the neighbourhood \mathcal{U} of Γ , hence $\mu_2 < 0$. This ensures that there exists a connection formed by separatrix Γ_1 from pq_1 to itself. If we set $\mu_3 < -a_2 T_{34}(\mu_2)$, the non-central connection from pq_1 to itself will become central. In this case the separatrix Γ_1 forms a SNIC that enters the neighbourhood of pq_1 from central direction direction. The other way around $\mu_3 > -a_2 T_{34}(\mu_2)$ ensures the persistence of the limit cycle in the system and the separatrix Γ_1 stays in the neighbourhood \mathcal{U} tending to the periodic orbit.

4.1.4 Birth and death of periodic solutions

We can conclude that in the parameter space μ_2 and μ_3 with $\mu_1 = 0$ SNIC bifurcation, together with homoclinic bifurcation and SNICeroclinic bifurcation, govern the transition from the persistence of the periodic orbit solutions in the system to the trajectories leaving the neighbourhood \mathcal{U} via the separatrix Γ_1 . In the later case $\mu_3 < 0$ allows to maintain central heteroclinic connection $p_2 \rightarrow pq_1$, while for $\mu_3 > 0$ the connection is broken. In the parameter space where the periodic solutions exist the choice of the parameters decides the the qualitative behaviour of the separatrices and their interactions with the periodic orbit. Namely, if we are in the second quadrant ($\mu_2 < 0$ and

$\mu_3 > 0$), both separatrices will tend to the periodic orbit. If we cross the threshold and enter the first quadrant ($0 < \mu_2 < -a_1 T_{12}(\mu_3)$), Γ_2 continues to tend to the periodic orbit, while Γ_1 leaves the neighbourhood. Likewise crossing the threshold of the third quadrant ($-a_2 T_{34}(\mu_2) < \mu_3 < 0$) maintains the tendency of Γ_1 to the periodic orbit, while Γ_2 forms a central connection from p_2 to p_{q1} .

4.2 Changes in the qualitative dynamics with one hyperbolic saddle ($\mu_1 < 0$)

When the parameter $\mu_1 < 0$ the system has gone through the saddle-node bifurcation and saddle-node p_{q1} disappears together with the separatrix Γ_1 . As a result the system has only one equilibrium, which is a saddle point p_2 . Now varying the parameters μ_2 and μ_3 we only need to consider the bifurcations of the separatrix Γ_2 .

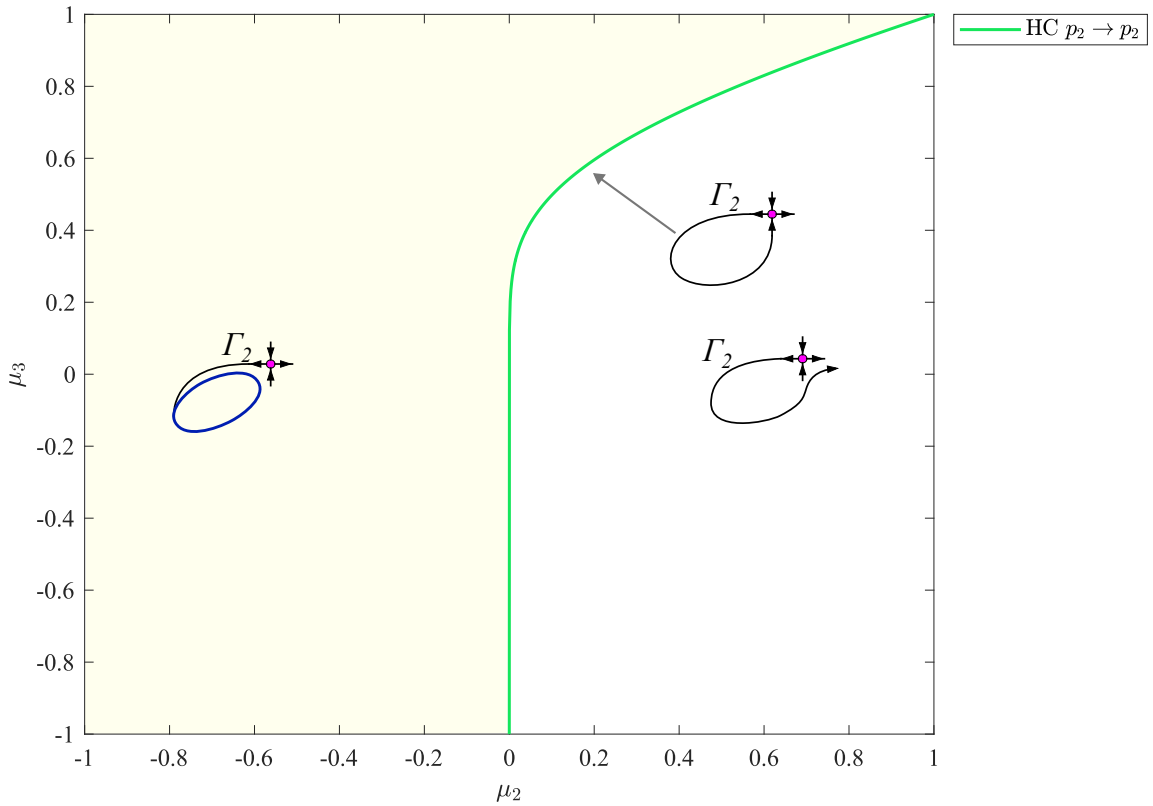


Figure 7: The unfolding of the SNICeroclinic loop for negative $\mu_1 = -0.1$ in the parameters μ_2 and μ_3 . The green line depicts the homoclinic curve for. Left (right) to the homoclinic curve in the yellow (white) region we have persistence (destruction) of the periodic solutions. The sketches of the phase portraits illustrate the qualitative behaviour of the system, depicting the behaviour of the separatrices Γ_1 and Γ_2 . There the pink dot identifies hyperbolic saddle equilibrium, while dark blue closed loop shows the presence of the periodic orbits.

First, we consider the conditions for the persistence of the homoclinic loop with p_2 . The condi-

tions are similar to the ones discussed in subsection 4.1.2, i.e. the fixed point of the return map R_3 must be zero, as result we get the expression for the parameter μ_2 in terms of μ_3 :

$$\mu_2 = -a_1 T_{12}(\mu_3). \quad (59)$$

Unlike $\mu = 0$ case, we do not need to restrict the values of μ_3 as there is no other point for the separatrix Γ_2 to interact with. The connection map in Equation 59 depends on parameter μ_1 , altering the position of the homoclinic curve in the parameter space (μ_2, μ_3) with the changes of μ_1 (Figure 7). If $\mu_2 < -a_1 T_{12}(\mu_3)$ the separatrix Γ_2 stays in the neighbourhood \mathcal{U} without passing through p_2 , which identifies the presence of the periodic solutions. Otherwise, when $\mu_2 > -a_1 T_{12}(\mu_3)$ the separatrix Γ_2 leaves the neighbourhood \mathcal{U} , as a result there are no invariant objects present. In summary, when $\mu_1 > 0$ the system can only be in three states: persistence of the periodic solutions, homoclinic loop with p_2 , which then serves as a mechanism of the periodic solution destruction.

4.3 Changes in the qualitative dynamics with two hyperbolic saddles ($\mu_1 > 0$)

Finally, we discuss the case when $\mu_1 > 0$ where there are two hyperbolic equilibria p_1 and p_2 . When we vary the splitting parameters μ_2 and μ_3 we can observe a range of different dynamic behaviours that arise from different interactions of the separatrices Γ_1 and Γ_2 . We summarise all of the possible cases in the schematic in Figure 8. In the following subsections we discuss the conditions for each of the cases.

4.3.1 Persistence of the heteroclinic connections

As we fix $\mu_1 > 0$ the saddle-node becomes a saddle equilibrium and changes its location in the phase space. Specifically, the location of the saddle point on the cross-section Σ_1 is $x = \sqrt{\mu_1}$. To preserve the heteroclinic loop we need to move the separatrix Γ_2 so that the flow hits Σ_1 at $x = \sqrt{\mu_1}$. It can be achieved by setting the splitting parameter $\mu_3 = \sqrt{\mu_1}$. The maps R_2, R_3, R_4 will have a stable fixed point at $x = 0$, while R_1 's stable fixed point will be at $x = \sqrt{\mu_1}$, indicating bidirectional heteroclinic connection. What is more, fixing $\mu_3 = \sqrt{\mu_1}$ and varying $\mu_2 \neq 0$ we preserve the heteroclinic connection $p_2 \rightarrow p_1$, formed by the separatrix Γ_2 . However, for $\mu_2 < 0$ the separatrix Γ_1 tends to the periodic orbit, while for $\mu_2 > 0$ it leaves the neighbourhood \mathcal{U} (see Figure 8). On the other hand, if we fix $\mu_2 = 0$ and vary the splitting parameter μ_3 we only preserve the heteroclinic connection $p_1 \rightarrow p_2$, formed by the separatrix Γ_1 . The separatrix Γ_2 either tends to the periodic orbit for $\mu_3 > \sqrt{\mu_1}$ or leaves the neighbourhood \mathcal{U} for $\mu_3 < \sqrt{\mu_1}$.

4.3.2 Homoclinic loop $p_1 \rightarrow p_1$

As we have two saddle equilibria we have a possibility for two distinct homoclinic loop - $p_1 \rightarrow p_1$ and $p_2 \rightarrow p_2$. In the first case we need to ensure the intersection of the stable and unstable manifolds of the saddle p_1 . For that we require that the trajectories in the neighbourhood \mathcal{U} are to enter the cross-section Σ_1 at a point $(\sqrt{\mu_1}, \epsilon)$, where the location of the saddle equilibrium is, so the return map R_1 has to have a fixed point at $x = \sqrt{\mu_1}$:

$$0 = R_1(\sqrt{\mu_1}) - \sqrt{\mu_1} \quad (60)$$

$$0 = a_2 T_{34}(\mu_2) + \mu_3 - \sqrt{\mu_1} \quad (61)$$

$$\mu_3 = -a_2 T_{34}(\mu_2) + \sqrt{\mu_1}. \quad (62)$$

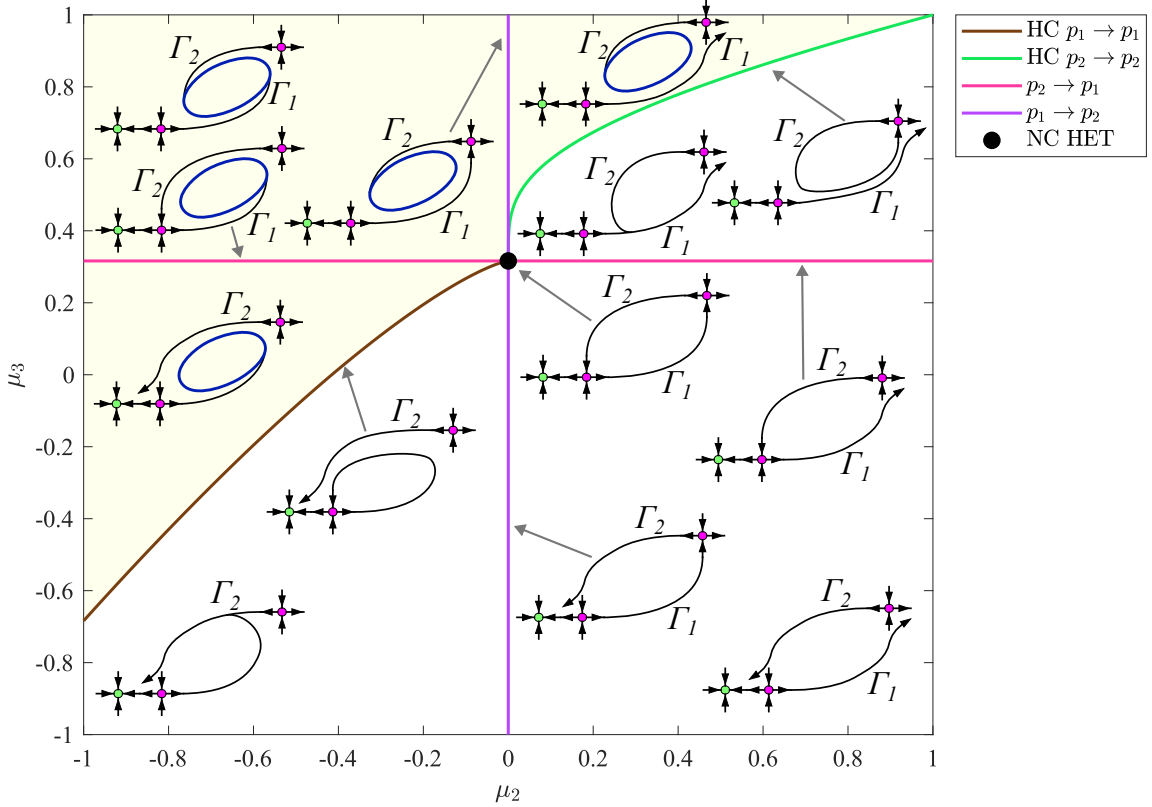


Figure 8: Unfolding of the SNICeroclinic loop for $\mu_1 > 0$, when two hyperbolic (pink dots) equilibria present. The green dot identifies a stable node near saddle equilibria p_1 . The parameter $\mu_1 = 0.1$ is fixed, while changes in parameters μ_2 and μ_3 alter the qualitative behaviour of the system. Black dot signifies the heteroclinic loop between the two equilibria, the curves separate the parameter regions of different dynamics as described in the legend. Yellow and white coloured regions signify the presence and absence of a periodic orbit, respectively. The dynamics of the system is also illustrated via phase portraits, depicting the behaviour of the separatrices Γ_1 and Γ_2 . Dark blue closed curves identify the presence of a periodic orbit. HC: homoclinic loop, HET: hetroclinic loop.

Additionally, we require the separatrix Γ_1 not to leave the neighbourhood \mathcal{U} , hence $\mu_2 < 0$. This ensures there exists a homoclinic connection $p_1 \rightarrow p_1$. The separatrix Γ_2 leaves the neighbourhood \mathcal{U} . Setting $\mu_3 > -a_2 T_{34}(\mu_2) + \sqrt{\mu_1}$ leads to the existence of a periodic solution in the system. Specifically, the separatrix Γ_1 tends to a periodic orbit, while Γ_2 leaves the neighbourhood as before. In the case when $\mu_3 < -a_2 T_{34}(\mu_2) + \sqrt{\mu_1}$ the stable point in the return map R_1 disappears, indicating that the separatrix Γ_1 overlaps with Γ_2 and leaves the neighbourhood \mathcal{U} . Thus the surface $\mu_3 < -a_2 T_{34}(\mu_2) + \sqrt{\mu_1}$ indicated a mechanism of birth and destruction of periodic orbits in the system.

4.3.3 Homoclinic loop $p_2 \rightarrow p_2$

The conditions for the second homoclinic loop $p_2 \rightarrow p_2$ require the intersection of the stable and unstable manifolds of the saddle point p_2 , hence the return map R_3 needs to have a stable point at

$x = 0$, as was discussed in subsection 4.1.2 and subsection 4.2:

$$\mu_2 = -a_1 T_{12}(\mu_3). \quad (63)$$

Moreover, we need to impose the condition for Γ_2 not to leave the neighbourhood \mathcal{U} , thus $\mu_3 > \sqrt{\mu_1}$. Under these conditions the separatrix Γ_2 forms a homoclinic loop with p_2 , and the separatrix Γ_1 leaves the neighbourhood \mathcal{U} . If we set $\mu_2 < -a_1 T_{12}(\mu_3)$ the separatrix Γ_2 stays in the neighbourhood \mathcal{U} but does not go through p_2 , hence it tends to a periodic orbit. Otherwise if $\mu_2 > -a_1 T_{12}(\mu_3)$, the return map R_3 does not have a stable fixed point, indicating that the separatrix Γ_2 overlaps with Γ_1 and leaves the neighbourhood \mathcal{U} . Here surface $\mu_2 = -a_1 T_{12}(\mu_3)$ acts as a threshold for a transition from periodic solutions to their disappearance via a homoclinic loop with p_2 .

4.3.4 Periodic solutions: their birth and destruction

After considering the persistence of homoclinic loops with p_1 and p_2 as well as the heteroclinic loop $p_1 \leftrightarrow p_2$ in the system, we identify the following mechanisms governing the birth and death of the periodic solutions in the system for $\mu_1 > 0$. For $\mu_1 > 0$ the periodic orbits can be born/destroyed via one of the following mechanisms: homoclinic bifurcation with p_1 , homoclinic bifurcation with p_2 , heteroclinic connection $p_1 \leftrightarrow p_2$. Depending on the transition mechanism (whether it is a homoclinic bifurcation with p_1 or p_2), the flow, that originates in the neighbourhood \mathcal{U} , could leave \mathcal{U} from different sides. We remark that the above holds for Type I (and on time-reversal Type IV) but for Types II and III saddle-nodes bifurcations of periodic orbits (SNIPER) will appear [26], as in this case the periodic orbits emerging at the homoclinic bifurcations with p_1 and p_2 will be of different stabilities. Specifically, one will give rise to a stable limit cycle, and the other one will make an unstable one. Moreover, if the parameters are such that $\mu_2 < 0$ and $\mu_3 > \sqrt{\mu_1}$, both separatrices tend to the limit cycle. On the other hand, if $\mu_2 > 0$ and $\mu_3 < \sqrt{\mu_1}$, both separatrices leave the neighbourhood \mathcal{U} . This illustrates various global mechanisms responsible for birth and destruction of periodic solutions in dynamical system settings. Specifically, changes in the parameters μ_2 and μ_3 can lead to the convergence of the solutions to various attractors under the perturbations to the limit cycle.

5 Discussion

In this paper we propose definitions for (non-central) SNICeroclinic loops and present a generic unfolding of the non-central SNICeroclinic loop in the plane. This is a codimension-three bifurcation of a heteroclinic loop between a saddle and a saddle-node. Our analysis augments previous work on the saddle-node homoclinic loop unfolding [17–19], that governs the transition from a homoclinic-born and -destroyed oscillations to oscillations born and destroyed via a SNIC. Our work parallels that in [25, 26]. We highlight that the unfolding in this scenario includes saddle-node local bifurcation as well as heteroclinic, homoclinic and SNIC global bifurcations.

We suggest a classification of different types of planar non-central SNICeroclinic, while the focus of unfolding is on Type I. This is the most stable case (the saddle-node has linearly stable eigenvalue and the saddle is dominantly stable), and we give an example of Type I in section 2. We also provide an example in section 2 of Type IV that we identified in a GTPase activation model [20, 29]. The unfolding of mixed cases Type II and III can be found in the work of [26] who show that, in addition to the unfolding structure that we have identified in Type I, Type II and III also feature a SNIPER (saddle-node of periodic orbits) curve, where stable and unstable periodic orbits meet. The SNIPER bifurcation has been identified as a route to hidden attractors both theoretically and experimentally

in electronic circuits [36]. Its interaction with the SNICeroclinic bifurcation suggests new dynamical structures that may be interesting from both theoretical and experimental perspectives.

5.1 Extensions to higher dimensions

The minimal dimensionality that allows the presence of the SNICeroclinic loop is two. As with Schechter's work on the SNHL in the planar case [17] that was extended to higher dimensions in [18, 19], we highlight that there is a significant task to extend the analysis here to unfolding general non-central SNICeroclinic loops in a higher-dimensional system.

The unfolding of the heteroclinic loop between non-hyperbolic and hyperbolic saddle equilibria, where the non-hyperbolic equilibrium is assumed to undergo a transcritical bifurcation, for a 4-dimensional system is presented in [37]. Further work considers the case of non-generic heteroclinic loop with non-hyperbolic equilibria [38]. Some other methods unfolding heteroclinic loops in higher-dimensional systems can be found in [24, 35, 39, 40].

For $n > 2$ there will be many types of SNICeroclinic loop in Equation 7 that need to be considered for a complete classification. In particular, note **H1*** means that p_{q1} has either a center-stable, or a center-unstable, manifold of dimension n . The saddle p_2 also has several choices for invariant manifold dimension

$$\dim W^s(p_2) = k_s \geq 1, \quad \dim W^u(p_2) = k_u \geq 1,$$

such that $k_s + k_u = n$. The simplest cases (parallel to Types I and IV in Table 1) will be where $W^{cs}(p_{q1}) = n$, $k_u = 1$, Γ_2 approaches in non-central direction (Type I/II) and where $W^{cu}(p_{q1}) = 2$, $k_s = 1$, Γ_1 leaves in non-central direction (Type III/IV), and this will also be present at codimension three. Even in these cases the unfolding may be richer due for example to strong and weak directions of attraction/repulsion, and due to rotations due to complex eigenvalues. More general cases (in particular hetero-dimensional cases) will typically have higher codimension but the presence of multiple connections will give much richer dynamical and bifurcation behaviour, as observed for heteroclinic cycles between saddles [41].

5.2 Applications

Our recent analysis of a mathematical model of neural circuitry in the amygdalarevealed a heteroclinic loop between saddle-node and saddle [42]. This loop acts as a transition mechanism between a SNIC and a homoclinic orbit with distinct equilibria.

The analysis in the present paper has identified a range of qualitative dynamical behaviours, including central and non-central SNIC, periodic and homoclinic orbits as well as absence of invariant objects in the system. All of these behaviours stem from the non-central SNICeroclinic loop, highlighting its importance for induction of oscillatory dynamics. Specifically, non-central SNIC is exactly a SNHL bifurcation, that has been dubbed as the organizing center for multi-pulse excitability in lasers [4, 5].

Furthermore, perturbations to the excitable 1D medium gives rise to travelling pulses and the characteristics of their behaviour are mediated by the type of global bifurcation giving rise to oscillations [43]. Extending research in excitability in terms of SNICeroclinic loop can provide further theoretical insights in underlying mechanisms of excitability and travelling wave phenomena. It has previously been shown that a robust heteroclinic cycle can give rise to the family of periodic travelling waves, which is considered in Rock-Paper-Scissors model [44].

The SNICeroclinic can potentially be an organizing center for models depicting heteroclinic phenomenon. One potential candidate is the systems of coupled networks. In the model of identically

coupled phase oscillators, robust ‘slow switching’ oscillations originate from presence of robust heteroclinic attractors [45]. In the system of two-coupled active rotors with Kuramoto-type coupling [46], the switch between dissipative and conservative dynamics is governed by complex heteroclinic and homoclinic structures connecting the fixed points within and outside the symmetry subspace. presence of robust heteroclinic attractors.

The non-central heteroclinic between a saddle and a saddle-node, was previously described in the literature [26]. In this study, we reveal that this results in a rich variety of bifurcations of oscillations and speculate that including the SNICeroclinic in continuation toolboxes will be a practically useful addition to the various hyperbolic homoclinic and heteroclinic bifurcations that can be found, for example, using [47–49]. In particular, non-hyperbolic orbit continuation is a challenging task. Therefore, robust methods to numerically identify and continue the SNICeroclinic in continuation routines will be especially useful.

Data accessibility

The code to reproduce the analysis can be found in a github repository

Declaration of AI use

We have not used AI-assisted technologies in creating this article.

Conflict of interest declaration

The authors declare that they have no conflicts of interest.

Funding

KTA and PA gratefully acknowledge the financial support of the EPSRC via grant EP/T017856/1. KN is a PhD student funded by the EPSRC.

Disclaimer

For the purpose of open access, the author has applied a ‘Creative Commons Attribution (CC BY) licence to any Author Accepted Manuscript version arising.

Acknowledgements

We would like to acknowledge helpful comments and suggestions by Sebastian Wieczorek, Jan Sieber, and Claire Postlethwaite.

References

- [1] Andrey Shilnikov, G Nicolis, and C Nicolis. “Bifurcation and Predictability Analysis of a Low-Order Atmospheric Circulation Model”. In: *International Journal of Bifurcation and Chaos* 5 (Dec. 1995), pp. 1701–1711. DOI: 10.1142/S0218127495001253.
- [2] Eoin O’Sullivan, Kieran Mulchrone, and Sebastian Wieczorek. “Rate-induced tipping to metastable Zombie fires”. EN. In: *Proceedings of the Royal Society A* (June 2023). Publisher: The Royal Society. DOI: 10.1098/rspa.2022.0647. URL: <https://royalsocietypublishing.org/doi/10.1098/rspa.2022.0647> (visited on 11/03/2024).
- [3] A. L. Shil’nikov. “Homoclinic phenomena in laser models”. In: *Computers & Mathematics with Applications* 34.2 (July 1997), pp. 245–251. ISSN: 0898-1221. DOI: 10.1016/S0898-1221(97)00126-0. URL: <https://www.sciencedirect.com/science/article/pii/S0898122197001260> (visited on 11/03/2024).
- [4] Sebastian Wieczorek and Bernd Krauskopf. “Bifurcations of n-homoclinic orbits in optically injected lasers”. en. In: *Nonlinearity* 18.3 (Feb. 2005), p. 1095. ISSN: 0951-7715. DOI: 10.1088/0951-7715/18/3/010. URL: <https://dx.doi.org/10.1088/0951-7715/18/3/010> (visited on 11/03/2024).
- [5] Bernd Krauskopf et al. “Excitability and self-pulsations near homoclinic bifurcations in semiconductor laser systems”. en. In: *Optics Communications* 215.4-6 (Jan. 2003), pp. 367–379. ISSN: 00304018. DOI: 10.1016/S0030-4018(02)02239-3. URL: [https://linkinghub.elsevier.com/retrieve/pii/S00304018\(02\)02239-3](https://linkinghub.elsevier.com/retrieve/pii/S00304018(02)02239-3) (visited on 10/15/2024).
- [6] Christian Kaas-Petersen and Stephen K. Scott. “Homoclinic orbits in a simple chemical model of an autocatalytic reaction”. In: *Physica D: Nonlinear Phenomena* 32.3 (Dec. 1988), pp. 461–470. ISSN: 0167-2789. DOI: 10.1016/0167-2789(88)90069-3. URL: <https://www.sciencedirect.com/science/article/pii/0167278988900693> (visited on 11/03/2024).
- [7] B. Kazmierczak and T. Lipniacki. “Homoclinic solutions in mechanical systems with small dissipation. Application to DNA dynamics”. eng. In: *Journal of Mathematical Biology* 44.4 (Apr. 2002), pp. 309–329. ISSN: 0303-6812. DOI: 10.1007/s002850100131.
- [8] Eugene M. Izhikevich. “NEURAL EXCITABILITY, SPIKING AND BURSTING”. en. In: *International Journal of Bifurcation and Chaos* 10.06 (June 2000), pp. 1171–1266. ISSN: 0218-1274, 1793-6551. DOI: 10.1142/S0218127400000840. URL: <https://www.worldscientific.com/doi/abs/10.1142/S0218127400000840> (visited on 08/27/2024).
- [9] Roberto Barrio et al. “Dynamics of excitable cells: spike-adding phenomena in action”. en. In: *SeMA Journal* 81.1 (Mar. 2024), pp. 113–146. ISSN: 2281-7875. DOI: 10.1007/s40324-023-00328-2. URL: <https://doi.org/10.1007/s40324-023-00328-2> (visited on 08/27/2024).
- [10] Manoj Aravind and Hildegard Meyer-Ortmanns. “On relaxation times of heteroclinic dynamics”. In: *Chaos: An Interdisciplinary Journal of Nonlinear Science* 33.10 (Oct. 2023), p. 103138. ISSN: 1054-1500. DOI: 10.1063/5.0166803. URL: <https://doi.org/10.1063/5.0166803> (visited on 08/27/2024).
- [11] Mikhail I. Rabinovich et al. “Information flow dynamics in the brain”. In: *Physics of Life Reviews* 9.1 (Mar. 2012), pp. 51–73. ISSN: 1571-0645. DOI: 10.1016/j.plrev.2011.11.002. URL: <https://www.sciencedirect.com/science/article/pii/S1571064511001448> (visited on 08/27/2024).
- [12] Pablo Varona and Mikhail I. Rabinovich. “Hierarchical dynamics of informational patterns and decision-making”. In: *Proceedings of the Royal Society B: Biological Sciences* 283.1832 (June 2016). Publisher: Royal Society, p. 20160475. DOI: 10.1098/rspb.2016.0475. URL: <https://royalsocietypublishing.org/doi/10.1098/rspb.2016.0475> (visited on 08/27/2024).

- [13] Valentin Afraimovich, Xue Gong, and Mikhail Rabinovich. “Sequential memory: Binding dynamics”. In: *Chaos: An Interdisciplinary Journal of Nonlinear Science* 25.10 (Oct. 2015), p. 103118. ISSN: 1054-1500. DOI: 10.1063/1.4932563. URL: <https://doi.org/10.1063/1.4932563> (visited on 08/27/2024).
- [14] Mikhail I. Rabinovich, Irma Tristan, and Pablo Varona. “Hierarchical nonlinear dynamics of human attention”. In: *Neuroscience & Biobehavioral Reviews* 55 (Aug. 2015), pp. 18–35. ISSN: 0149-7634. DOI: 10.1016/j.neubiorev.2015.04.001. URL: <https://www.sciencedirect.com/science/article> (visited on 08/27/2024).
- [15] John Guckenheimer. “Multiple bifurcation problems for chemical reactors”. In: *Physica D: Nonlinear Phenomena* 20.1 (May 1986), pp. 1–20. ISSN: 0167-2789. DOI: 10.1016/0167-2789(86)90093-X. URL: <https://www.sciencedirect.com/science/article/pii/016727898690093X> (visited on 09/26/2024).
- [16] V. I. Luk’yanov. “Bifurcations of dynamical systems with a saddle-point-separatrix loop”. In: *Differentsial’nye Uravneniya (J. Differential Equations)* 18 (1982), 1493–1506 (1049–1059).
- [17] Stephen Schecter. “The Saddle-Node Separatrix-Loop Bifurcation”. In: *SIAM J. Math. Anla.* 18 (July 1987), pp. 1142–1157. DOI: 10.1137/0518083.
- [18] Shui-Nee Chow and Xiao-Biao Lin. “Bifurcation of a homoclinic orbit with a saddle-node equilibrium”. In: *Differential and Integral Equations* 3.3 (Jan. 1990). Publisher: Khayyam Publishing, Inc., pp. 435–466. ISSN: 0893-4983. URL: <https://projecteuclid.org/journals/differential-and-integ> (visited on 08/27/2024).
- [19] Bo Deng. “HOMOCLINIC BIFURCATIONS WITH NONHYPERBOLIC EQUILIBRIA”. In: *Department of Mathematics: Faculty Publications* (May 1989). URL: <https://digitalcommons.unl.edu/mathfac>
- [20] Cole Zmurchok et al. “Local and Global Bifurcations in a Mechanochemical ODE Model for Cell Behavior”. en. In: *Differential Equations and Dynamical Systems* (Mar. 2023). ISSN: 0971-3514, 0974-6870. DOI: 10.1007/s12591-023-00636-z. URL: <https://link.springer.com/10.1007/s12591-023> (visited on 10/10/2024).
- [21] Rui Dilão and Andrés Volford. “Excitability in a model with a saddle-node homoclinic bifurcation”. en. In: *Discrete and Continuous Dynamical Systems - B* 4.2 (Feb. 2004). Publisher: Discrete and Continuous Dynamical Systems - B, pp. 419–434. ISSN: 1531-3492. DOI: 10.3934/dcdsb.2004.4.419. URL: <https://www.aims sciences.org/en/article/doi/10.3934/dcdsb.2004.4.419> (visited on 11/03/2024).
- [22] Mark Borisuk et al. “Bifurcation Analysis of a Model of the Frog Egg Cell Cycle by”. In: (Dec. 2008).
- [23] Yuya Maruyama, Yuta Kakimoto, and Osamu Araki. “Analysis of chaotic oscillations induced in two coupled Wilson-Cowan models”. eng. In: *Biological Cybernetics* 108.3 (June 2014), pp. 355–363. ISSN: 1432-0770. DOI: 10.1007/s00422-014-0604-8.
- [24] Ale Jan Homburg and Björn Sandstede. “Chapter 8 - Homoclinic and Heteroclinic Bifurcations in Vector Fields”. In: *Handbook of Dynamical Systems*. Ed. by H. W. Broer, B. Hasselblatt, and F. Takens. Vol. 3. Elsevier Science, Jan. 2010, pp. 379–524. DOI: 10.1016/S1874-575X(10)00316-4. URL: <https://www.sciencedirect.com/science/article/pii/S1874575X10003164> (visited on 08/27/2024).
- [25] T.M. Grozovski. “Bifurcations of polycycles “apple“ and “half-apple” in typical two-parameter families”. In: *Differentsial’nye Uravneniya (J. Differential Equations)* 32.4 (1996), pp. 458–469.

- [26] F. Dumortier, R. Roussarie, and C. Rousseau. “Elementary graphics of cyclicity 1 and 2”. en. In: *Nonlinearity* 7.3 (May 1994), p. 1001. ISSN: 0951-7715. DOI: 10.1088/0951-7715/7/3/013. URL: <https://dx.doi.org/10.1088/0951-7715/7/3/013> (visited on 11/04/2024).
- [27] LP Shilnikov et al. *Methods of Qualitative Theory in Nonlinear Dynamics: (Part II)*. Sept. 2001. ISBN: 978-981-02-4072-1. DOI: 10.1142/4221.
- [28] Henri Poincaré and Bruce Popp. *The Three-Body Problem and the Equations of Dynamics*. Vol. 443. Jan. 2017. ISBN: 978-3-319-52898-4. DOI: 10.1007/978-3-319-52899-1.
- [29] Cole Zmurchok, Dhananjay Bhaskar, and Leah Edelstein-Keshet. “Coupling mechanical tension and GTPase signaling to generate cell and tissue dynamics”. en. In: *Physical Biology* 15.4 (Apr. 2018). Publisher: IOP Publishing, p. 046004. ISSN: 1478-3975. DOI: 10.1088/1478-3975/aab1c0. URL: <https://dx.doi.org/10.1088/1478-3975/aab1c0> (visited on 10/10/2024).
- [30] Yuri A. Kuznetsov. *Elements of Applied Bifurcation Theory*. en. Vol. 112. Applied Mathematical Sciences. Cham: Springer International Publishing, 2023. ISBN: 978-3-031-22006-7 978-3-031-22007-4. DOI: 10.1007/978-3-031-22007-4. URL: <https://link.springer.com/10.1007/978-3-031-22007-4> (visited on 09/13/2024).
- [31] H. W. Broer and F. Takens. “Chapter 1 - Preliminaries of Dynamical Systems Theory”. In: *Handbook of Dynamical Systems*. Ed. by H. W. Broer, B. Hasselblatt, and F. Takens. Vol. 3. Elsevier Science, Jan. 2010, pp. 1–42. DOI: 10.1016/S1874-575X(10)00309-7. URL: <https://www.sciencedirect.com/science/article/pii/S1874575X10003097> (visited on 08/29/2024).
- [32] J. Carr. *Applications of Centre Manifold Theory: 35*. English. 1982nd edition. New York Heidelberg: Kluwer Academic Publishers, June 1981. ISBN: 978-0-387-90577-8.
- [33] G. B. Ermentrout and N. Kopell. “Parabolic Bursting in an Excitable System Coupled with a Slow Oscillation”. In: *SIAM Journal on Applied Mathematics* 46.2 (1986). Publisher: Society for Industrial and Applied Mathematics, pp. 233–253. ISSN: 0036-1399. URL: <https://www.jstor.org/stable/21> (visited on 08/29/2024).
- [34] C. Baesens and R. S. MacKay. “Interaction of two systems with saddle-node bifurcations on invariant circles: I. Foundations and the mutualistic case”. en. In: *Nonlinearity* 26.12 (Nov. 2013). Publisher: IOP Publishing, p. 3043. ISSN: 0951-7715. DOI: 10.1088/0951-7715/26/12/3043. URL: <https://dx.doi.org/10.1088/0951-7715/26/12/3043> (visited on 08/29/2024).
- [35] Mikhail V. Shashkov and Dmitry V. Turaev. “ON THE COMPLEX BIFURCATION SET FOR A SYSTEM WITH SIMPLE DYNAMICS”. en. In: *International Journal of Bifurcation and Chaos* 06.05 (May 1996), pp. 949–968. ISSN: 0218-1274, 1793-6551. DOI: 10.1142/S0218127496000527. URL: <https://www.worldscientific.com/doi/abs/10.1142/S0218127496000527> (visited on 08/29/2024).
- [36] Suresh Kumarasamy et al. “Saddle-node bifurcation of periodic orbit route to hidden attractors”. In: *Physical Review E* 107.5 (May 2023). Publisher: American Physical Society, p. L052201. DOI: 10.1103/PhysRevE.107.L052201. URL: <https://link.aps.org/doi/10.1103/PhysRevE.107.L052201> (visited on 11/06/2024).
- [37] Fengjie Geng, Dan Liu, and Deming Zhu. “BIFURCATIONS OF GENERIC HETEROCLINIC LOOP ACCOMPANIED BY TRANSCRITICAL BIFURCATION”. en. In: *International Journal of Bifurcation and Chaos* 18.04 (Apr. 2008), pp. 1069–1083. ISSN: 0218-1274, 1793-6551. DOI: 10.1142/S0218127408020847. URL: <https://www.worldscientific.com/doi/abs/10.1142/S0218127408020847> (visited on 09/05/2024).

- [38] Fengjie Geng et al. “Bifurcations of a nongeneric heteroclinic loop with nonhyperbolic equilibria”. en. In: *Discrete and Continuous Dynamical Systems - B* 18.1 (Sept. 2012). Publisher: Discrete and Continuous Dynamical Systems - B, pp. 133–145. ISSN: 1531-3492. DOI: 10.3934/dcdsb.2013.18.133. URL: <https://www.aims sciences.org/en/article/doi/10.3934/dcdsb.2013.18.133> (visited on 09/05/2024).
- [39] Deming Zhu and Zhihong Xia. “Bifurcations of heteroclinic loops”. en. In: *Science in China Series A: Mathematics* 41.8 (Aug. 1998), pp. 837–848. ISSN: 1862-2763. DOI: 10.1007/BF02871667. URL: <https://doi.org/10.1007/BF02871667> (visited on 09/19/2024).
- [40] Yinlai Jin and Deming Zhu. “Bifurcations of rough heteroclinic loop with two saddle points”. en. In: *Science in China Series A: Mathematics* 46.4 (July 2003), pp. 459–468. ISSN: 1862-2763. DOI: 10.1007/BF02884018. URL: <https://doi.org/10.1007/BF02884018> (visited on 09/19/2024).
- [41] Christian Bonatti and Lorenzo J. Díaz. “ROBUST HETERODIMENSIONAL CYCLES AND -GENERIC DYNAMICS”. en. In: *Journal of the Institute of Mathematics of Jussieu* 7.3 (July 2008), pp. 469–525. ISSN: 1475-3030, 1474-7480. DOI: 10.1017/S1474748008000030. URL: <https://www.cambridge.org/core/journals/journal-of-the-institute-of-mathematics-of-jussieu/article/doi/10.1017/S1474748008000030> (visited on 11/17/2024).
- [42] Kateryna Nechyporenko et al. “Neuronal network dynamics in the posterodorsal amygdala: shaping reproductive hormone pulsatility”. In: *Journal of The Royal Society Interface* 21.217 (Aug. 2024). Publisher: Royal Society, p. 20240143. DOI: 10.1098/rsif.2024.0143. URL: <https://royalsocietypublishing.org/doi/full/10.1098/rsif.2024.0143> (visited on 09/05/2024).
- [43] Pablo Moreno-Spiegelberg et al. “Bifurcation structure of traveling pulses in type-I excitable media”. In: *Physical Review E* 106.3 (Sept. 2022). Publisher: American Physical Society, p. 034206. DOI: 10.1103/PhysRevE.106.034206. URL: <https://link.aps.org/doi/10.1103/PhysRevE.106.034206> (visited on 10/15/2024).
- [44] Cris R. Hasan et al. “Spatiotemporal stability of periodic travelling waves in a heteroclinic-cycle model”. en. In: *Nonlinearity* 34.8 (July 2021). Publisher: IOP Publishing, p. 5576. ISSN: 0951-7715. DOI: 10.1088/1361-6544/ac0126. URL: <https://dx.doi.org/10.1088/1361-6544/ac0126> (visited on 11/04/2024).
- [45] Peter Ashwin, Oleksandr Burylko, and Yuri Maistrenko. “Bifurcation to heteroclinic cycles and sensitivity in three and four coupled phase oscillators”. In: *Physica D: Nonlinear Phenomena* 237.4 (Apr. 2008), pp. 454–466. ISSN: 0167-2789. DOI: 10.1016/j.physd.2007.09.015. URL: <https://www.sciencedirect.com/science/article/pii/S0167278907003454> (visited on 11/06/2024).
- [46] Oleksandr Burylko et al. “Time-reversible dynamics in a system of two coupled active rotators”. en. In: *Proceedings of the Royal Society A: Mathematical, Physical and Engineering Sciences* 479.2278 (Oct. 2023), p. 20230401. ISSN: 1364-5021, 1471-2946. DOI: 10.1098/rspa.2023.0401. URL: <https://royalsocietypublishing.org/doi/10.1098/rspa.2023.0401> (visited on 10/01/2024).
- [47] Romain Veltz. *{BifurcationKit.jl}*. 2020. URL: <https://hal.archives-ouvertes.fr/hal-02902346>.
- [48] E Doedel et al. *AUTO-07P: continuation and bifurcation software for ordinary differential equations*. 2007. URL: <http://indy.cs.concordia.ca/auto/>.
- [49] Virginie De Witte et al. “Interactive Initialization and Continuation of Homoclinic and Heteroclinic Orbits in MATLAB”. In: *ACM Trans. Math. Softw.* 38.3 (Apr. 2012), 18:1–18:34. ISSN: 0098-3500. DOI: 10.1145/2168773.2168776. URL: <https://dl.acm.org/doi/10.1145/2168773.2168776> (visited on 11/06/2024).